P1.45

SPECTRAL RETRIEVAL OF LATENT HEATING PROFILES FROM TRMM PR DATA: ALGORITHM DEVELOPMENT WITH A CLOUD-RESOLVING MODEL

Shoichi Shige[1,*], Yukari N. Takayabu[2], Wei-Kuo Tao[3], and Daniel E. Johnson[3,4]

[1]Earth Observation Research Center, National Space Development Agency of Japan, Tokyo, Japan
[2]Center for Climate System Research, University of Tokyo, Tokyo, Japan
[3]Laboratory for Atmospheres, NASA/Goddard Space Flight Center, Greenbelt, Maryland
[4]Goddard Earth Sciences and Technology Center, University of Maryland, Baltimore County, Baltimore, Maryland

1. INTRODUCTION

The spectral representation of rain profiles observed by the Precipitation Radar (PR) of the Tropical Rainfall Measuring Mission (TRMM) provides convective and stratiform rain characteristics over the equatorial area (Takayabu, 2002). Motivated by this, we introduce a new retrieval algorithm, the spectral latent heating (SLH) algorithm, for PR. The primary difference from three algorithms in Tao et al. (2001) is that we utilize rain profiles observed by PR.

2. METHOD

We produced a set of look-up tables for the SLH algorithm and tested its performance with the 2-D version of the Goddard Cumulus Ensemble (GCE) model (Tao and Simpson, 1993). Numerical simulations of cloud systems from December 10 1992 to January 4 1993 in TOGA COARE were conducted with observed large-scale forcing (Lin and Johnson, 1996). Convective and stratiform regions were identified using the GCE method, but non-surface precipitation regions were considered to be stratiform if rainfall rate aloft exceeded a threshold (0.3 mm h^{-1}).

The latent heating profiles are sorted referring to the precipitation top height (PTH) for convective and stratiform regions. Considering the sensitivity of PR, we used a threshold of 0.3 mm h^{-1} to determine PTH. Properties of convective heating profiles show near monotonic change with PTH (Fig. 1a). Stratiform heating profiles consist of two groups. One group consists of shallow stratiform heating profiles (PTH $<$ 4.4 km), characterized by upper-level cooling and low-level warming such as the tradewind cumulus regime (Nitta and Esbensen, 1974). The other

*Corresponding author address: Dr. Shoichi Shige, NASDA/Earth Observation Research Center, Harumi Island Triton Square, Office Tower X, 1-8-10 Harumi, Chuo-ku, Tokyo, 104-6023 Japan; e-mail: shige@eorc.nasda.go.jp

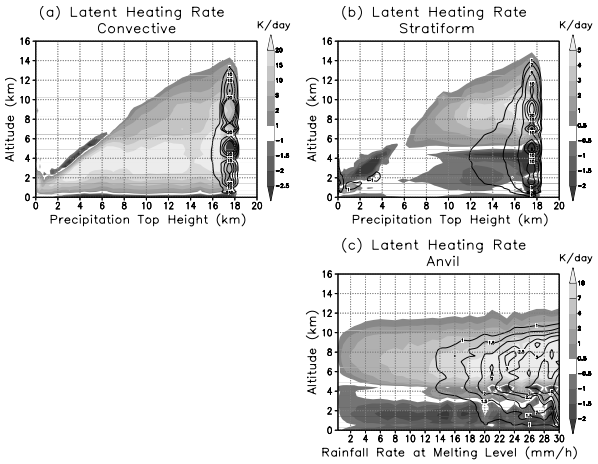

Figure 1: Model-generated heating profiles, plotted as functions of precipitation top height (PTH) from convective (a) and stratiform (b) regions, and rain fall rates at melting level from anvil region (c). Contours indicate values of confidence interval for the mean with the Student-t test.

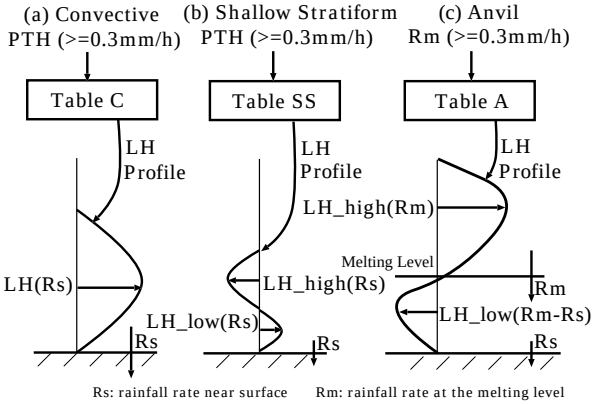

Figure 2: Diagram showing the procedure for deriving latent heating profiles using the spectral latent heating (SLH) algorithm.

group consists of anvil heating profiles (PTH $>$ 4.4 km), characterized by upper-level warming and low-level cooling. PR cannot correctly observe PTH for the anvil region because of the insensitivity of PR to the ice phase. Therefore, we use the rainfall rate at the melting level instead of PTH to produce the look-up table for the anvil region (Fig. 1c).

Figure 2 shows the procedure for deriving latent heating profiles using the SLH algorithm. For convective and shallow stratiform regions, the heating profiles corresponding to PTH are looked up in the tables. The amplitude is determined by the surface rainfall rate. For anvil, the heating profiles corresponding to the rainfall rate at the melting level are looked up in the table. The upper-level warming amplitude is then determined by the rainfall rate at the melting level. The lower-level cooling amplitude is determined by the difference of rainfall rate between the surface and the melting level.

3. PERFORMANCE

To test the performance of the SLH algorithm, we reconstructed latent heating profiles for December 19-27 1992, with the look-up tables shown in Fig. 1. The pattern in temporal variations of the simulated heating profile and the reconstructed one agree well (Fig. 3). The transitions among cloud system regimes (e.g., from the shallow convective stage to the mature stage during December 23-24) is realistically reconstructed – a key point for the use of TRMM latent heating estimates to improve the parameterization of convection in GCMs. This is a result of the utilization of observed information not only on precipitation type and intensity, but also on the precipitation depth. The heating profile in the decaying stage with no surface rain (e.g., December 25) can also be retrieved. This comes from utilizing the rain intensity at the melting level for anvil rain.

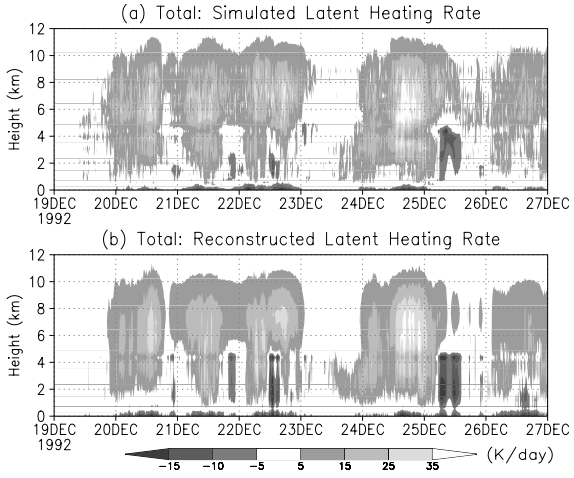

Figure 3: Time series of latent heating profiles for the period during December 19-27 1992. (a) Simulated from the GCE model. (b) Reconstructed using the SLH algorithm with the look-up tables shown in Fig. 1

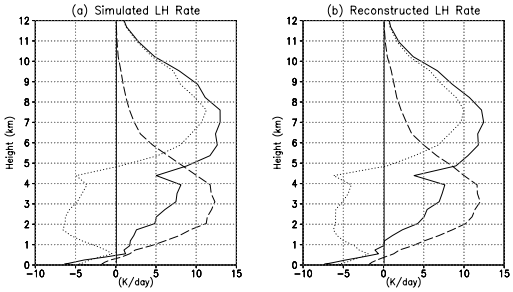

Figure 4: Eight-day average profiles of latent heating rate in total (solid), convective (dashed), and stratiform (dotted) regions. (a) Simulated from the GCE model. (b) Reconstructed using the SLH algorithm with the look-up tables shown in Fig. 1

The eight-day average profiles of the reconstructed latent heating agree very well with the simulated ones in total, convective and stratiform regions (Fig. 4). Some applications of the SLH algorithm to the TRMM PR data will be shown at the conference.

REFERENCES

Lin, X. and R. H. Johnson: 1996, Heating, moistening and rainfall over the western Pacific warm pool during TOGA COARE. *J. Atmos. Sci.*, **53**, 3367–3383.

Nitta, T. and S. Esbensen: 1974, Heat and moisture budget analyses using BOMEX data. *Mon. Wea. Rev.*, **102**, 17–28.

Takayabu, Y. N.: 2002, Spectral representation of rain features and diurnal variations observed with TRMM PR over the equatorial area. *Geophys. Res. Let.*, accepted.

Tao, W.-K., S. Lang, W. Olson, R. Meneghini, S. Yang, J. Simpson, C. Kummerow, E. Smith, and J. Halverson: 2001, Retrieved vertical profiles of latent heat release using TRMM rainfall products for February 1998. *J. Appl. Meteor.*, **40**, 957–982.

Tao, W.-K. and J. Simpson: 1993, Goddard cumulus ensemble model. Part I: Model description. *Terr. Atmos. Oceanic Sci.*, **4**, 35–72.